

ARTICLE

Extracellular Recording of Light Responses from Optic Nerve Fibers and the Caudal Photoreceptor in the Crayfish**Steven C. Nesbit¹, Alexander G. Van Hoof¹, Chi C. Le², & James R. Dearworth Jr.¹**¹*Biology Department and Neuroscience Program, Lafayette College, Easton, PA 18042;* ²*Department of Information Technology, Computer Science, and Digital Media, Juniata College, Huntingdon, PA 16652.*

Few laboratory exercises have been developed using the crayfish as a model for teaching how neural processing is done by sensory organs that detect light stimuli. This article describes the dissection procedures and methods for conducting extracellular recording from light responses of both the optic nerve fibers found in the animal's eyestalk and from the caudal photoreceptor located in the ventral nerve cord. Instruction for ADInstruments' data acquisition system is also featured for the data collection and analysis of responses. The comparison provides students a unique view on how spike activities measured from neurons code image-forming and non-image-forming processes. Results

from the exercise show longer latency and lower frequency of firing by the caudal photoreceptor compared to optic nerve fibers to demonstrate evidence of different functions. After students learn the dissection, recording procedure, and the functional anatomy, they can develop their own experiments to learn more about the photoreceptive mechanisms and the sensory integration of modalities by these light-responsive interneurons.

Key words: optic nerve fibers, caudal photoreceptors; Procambarus clarkii; Orconectes immunis; electrophysiology; extracellular recording

When introducing students to electrophysiological recording procedures in neuroscience, it is important to begin with a proper model. The crayfish is particularly useful because it is inexpensive and low maintenance. Being an invertebrate crustacean, there are no IACUC (Institutional Animal Care and Use Committee) regulations governing crayfish experimentation, allowing adoption for use in teaching laboratory courses (Welsh and Smith, 1960; Welsh et al., 1968; Deyrup-Olsen and Linder, 1991; Parfitt, 2002; Hauptman and Curtis, 2009; Wyttenbach et al., 2014; Johnson et al., 2014).

Other reasons for its selection include possession of a relatively simple nervous system and an ability to remain physiologically active *in vitro* (Wiersma, 1958; Wiersma and Hughes, 1961; Wiersma and Yamaguchi, 1966; Kondah and Hisada, 1986). Therefore, students can quickly learn the anatomy and carry out exercises to understand the principles of neurophysiology. Several instructional exercises have been developed using the crayfish to investigate the stretch receptor and synaptic integration at the neuromuscular junction in the tail segments (Parfitt, 2002; Mead et al., 2007; Hauptman and Curtis, 2009; Wyttenbach et al., 2014; Johnson et al., 2014); however, less has been developed that focuses on neural processing driven by light stimuli. These include an exercise that teaches undergraduates how to carry out electroretinogram recordings from the crayfish visual system (Olivo, 2003); and more recently, approaches for recording activities from caudal photoreceptors (Heitler, 2007; Johnson et al., 2015).

This paper is unique because it describes methods that use the crayfish to teach students how to extracellularly record spike activities of light responses from two types of visual interneurons: optic nerve fibers (Prosser, 1934; Naka and Kuwabara, 1959; Wiersma and Yamaguchi, 1966; Glantz, 2008) and the caudal photoreceptor

(Prosser, 1934; Welsh, 1934; Kennedy, 1963). Light-responsive optic nerve fibers belong to a subset of diverse interneurons found in the eyestalk that integrate image-forming light signals collected by the animal's compound eye (Meyer-Rochow, 2001). In contrast, functions of the caudal photoreceptor are non-image-forming and instead are thought to contribute to other light-evoked behaviors such as circadian rhythms (Kennedy, 1963; Rodríguez-Sosa et al., 2008) and backward walking (Edwards, 1984; Pei et al., 1996). The two cell bodies of the caudal photoreceptors are located in the sixth abdominal ganglion and send signals through their axons via the ventral nerve cord to the brain (Kennedy, 1963; Wilkens and Larimer, 1972, 1976). The dendrites, the light sensitive part of the caudal photoreceptor, project to the contralateral side of the ganglion.

Following the theme of the crayfish model, the dissections and recording procedures are relatively easy and provide students with a unique comparison of the light responses from very different photosensitive neurons found at the rostral and caudal ends of the animal.

MATERIALS AND METHODS**Animals**

Large crayfish, greater than or equal to 8.9 cm in length, were ordered from Carolina Biological Supply Company (Burlington, NC). The species type that is obtained depends on availability at the time of order; for this work, it was as mixture of *Procambarus clarkii* and *Orconectes immunis*, male and female. Other sources include seafood vendors; however, survivability can be compromised as they are delivered on ice and treated with the expectation of being consumed shortly after arrival.

Once received, the crayfish were maintained at room temperature in a 12:12 h light/dark cycle and were fed fish

food (Purina Aquamax for Sport Fish; Purina Mills, LCC, St. Louis, MO) twice per week. They were kept in separate containers with 3 cm deep room temperature dechlorinated water that was changed every week.

Recording Setup

Amplifier and Data Acquisition

Extracellular recordings were conducted inside a Faraday cage made of aluminum screens (65 x 80 x 80 cm) placed on top of a table. A heavy metal door salvaged from a defunct autoclave was placed on the table inside the cage and set on top of six tennis balls (12 cm in diameter; Petco Animal Supplies, Inc., San Diego, CA) to dampen vibrations. A tungsten microelectrode (WE30031.5A10; MicroProbes, Gaithersburg, MD), secured to a micromanipulator (Model M3301R; World Precision Instruments, Inc., Sarasota, FL), was used to record neural responses. Impedance of electrodes was 1.4–1.6 M Ω (cf. Prieto-Sagredo and Fanjul-Moles, 2001; Valdés-Fuentes et al., 2011). Properties of these electrodes included having a shaft diameter of 0.256 mm, which provided adequate support, and a tip (1 μ m) of medium tapered profile for reliable penetration through the connective tissue surrounding the optic nerve fibers (Wiersma and Yamaguchi, 1966). The microelectrode was connected to a P55 A.C. Pre-Amplifier (Grass-Telefactor, West Warwick, RI), which sent output to an ADInstruments PowerLab 26T data acquisition system connected to a PC running LabChart[®] v7.3.7 software. The P55 amplification was set to 1000X with the low filter cutoff set at 10 Hz and high cutoff at 3 kHz to isolate neural spikes. A RadioShack Mini Amplifier/speaker (Cat. No. 277-1008C; Tandy Corp., Fort Worth, TX) also received output from the amplifier to allow audible monitoring of the recordings.

Light stimulus

A white LED (light emitting diode) bulb (E27-W24-12V-WV; Super Bright LEDs Inc., St. Louis, MO) was used to evoke light responses. Using a radiometer (model DR-2000-LED; Gamma Scientific, San Diego, CA), radiant intensity from the light was measured at 2.56×10^{-4} W·sr⁻¹·cm⁻². The relative spectral radiance of the light is plotted in Figure 1. The LED bulb was placed 23 cm from the preparations and the timing of presentation was controlled using a Uniblitz[®] Electronic shutter (Vincent Associates, Rochester, NY). Open and closed states of the shutter were identified using the shutter driver, which sent a TTL (transistor-transistor logic) signal, accurate within 0.2 msec, to Channel 2 of the PowerLab. A 5 V signal indicated that the shutter was closed and a 0 V signal indicated that the shutter was open. Channel 2 was turned on in LabChart[®] and the scale was inverted so that the negative direction was up and the positive direction was down to make interpreting the shutter driver input more intuitive.

Dissections and Microelectrode Placements

Crayfish saline (5.4 mM KCl, 205 mM NaCl, 13.5 mM CaCl₂·2H₂O, 2.6 mM MgCl₂·6H₂O, 2.3 mM NaHCO₃, 2 mM

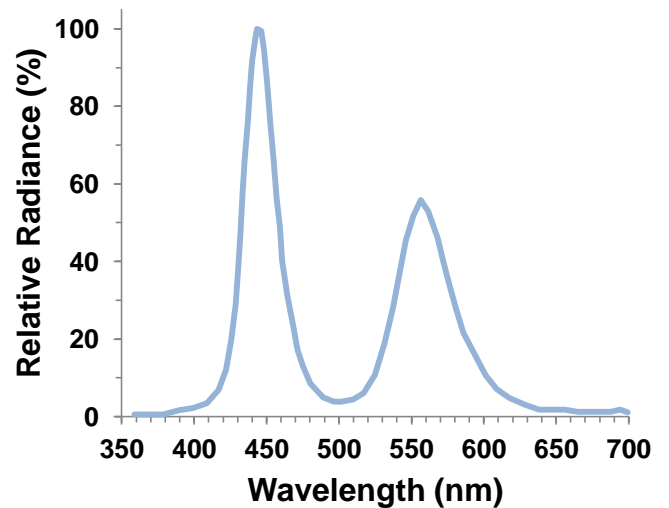


Figure 1. Relative spectral radiance for the white LED bulb re-plotted from data provided by Super Bright LEDs Inc. Cool white light (8000 K) made up of two broad spectral bands having peaks at 446 and 557 nm was emitted by 24 LEDs held in the bulb's base.

dextrose) was made to irrigate tissues during dissections (Van Harreveld, 1936; Wyttenbach et al., 2014). To prolong tissue survival during recordings (Aréchiga and Rodríguez-Sosa, 1998), the solution was chilled to 4 °C and bubbled continuously with a 95% O₂, 5% CO₂ mixture (234 cubic ft compressed gas cylinder; Airgas East, Inc., Salem, NH).

The crayfish were cryoanesthetized in ice for one hour before dissections (Gruhn and Rathmayer, 2002; Wyttenbach et al., 2014) in an opaque bucket to minimize activation of any light-responsive cells by ambient room lights (Video 1.1). The abdomen was separated from the thorax by making a cut at the rostral end of the first abdominal somite using dissection scissors (Fig. 2; Video 1.2). The thorax end was used for the dissection of the optic nerve fibers and the abdomen for dissection of the caudal photoreceptors. To maintain analgesia and to minimize movements, the sections were kept on ice during dissections.

A Leica Zoom 2000[™] stereoscope (Model No. Z30V; Leica Microsystems Inc., Buffalo, NY) was used to visualize the dissections. Lighting was provided by Lumina illuminators (Model No: FO-150; Chiu Technical Corporation, Kings Park, NY) with bifurcated fiber optic cables. One of the cable ends was covered with a Roscolux #65 Daylight Blue filter (Rosco Laboratories Inc., Stamford, CT) and was used during dissection of the optic nerve fibers. The filter was selected because it attenuates 520 to 680 nm light, to which the crayfish compound eye is thought to be most sensitive (Kennedy and Bruno, 1961). The purpose of the filter was to reduce bleaching of pigments that might occur prior to carrying out any recordings. The other cable end was covered with a Roscolux #318 Mayan Sun filter. This filter attenuates 420 to 580 nm light, to which the caudal photoreceptors are thought to be most sensitive (Uttal and Kasprzak, 1962).

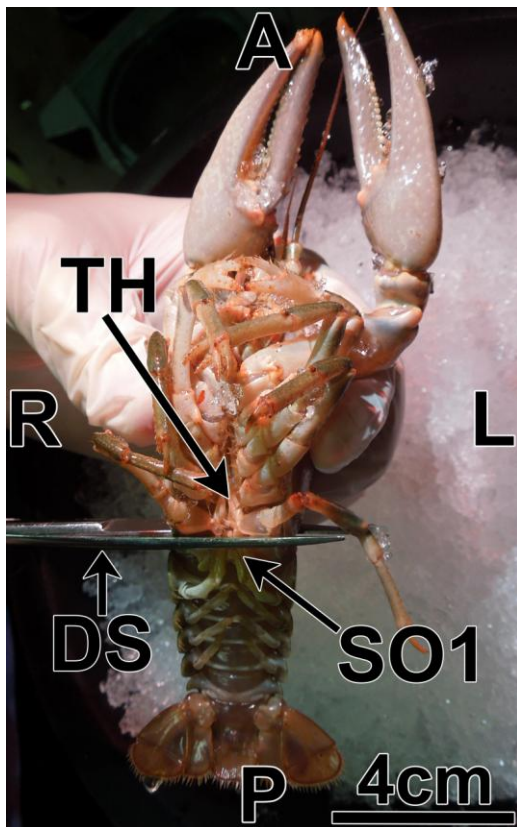


Figure 2. Ventral view of the crayfish showing abdomen removal. A, anterior; P, posterior; L, left; R, right; TH, thorax; SO1, first abdominal somite; DS, dissection scissors.

Optic Nerve Fibers

The thorax section was handled first to dissect and record from the optic nerve fibers. Small dissection scissors were used to make a lateral transverse cut of the rostrum just posterior to the eyestalk (Fig. 3A). The scissors were kept superficial to avoid damaging the eyestalk. A small lateral cut produced a fracture between the rostrum and the rest of the carapace. The rostrum then was removed by pulling the anterior end upward with forceps to expose the eyestalks (Fig. 3B; Video 1.3).

Any remaining carapace covering the eyestalk was removed using #5 Dumont forceps and microscissors. A Premiere® sterile surgical #11 blade (C&A Scientific, Manassas, VA) was used with the aid of the dissection stereoscope to sever one of the two joints connecting the ocular plate of the protocephalon with the basal sclerites of the eyestalk (Fig. 4). The cut was made by holding the blade at a shallow angle and moving the scalpel over the joint in the direction of the cutting edge (Video 1.4). Both medial- and lateral-facing scraping motions were carefully made to cut the joints, the underlying connective tissue, and the muscle of the eyestalks while staying superficial to the optic nerve. Crayfish saline was used to irrigate the eyestalks and the exposed optic nerve to prolong neural activity.

A pin reference electrode was inserted into the flexor muscle of the abdomen at the exposed caudal end of the thorax (where the abdomen was removed; Video 1.5)

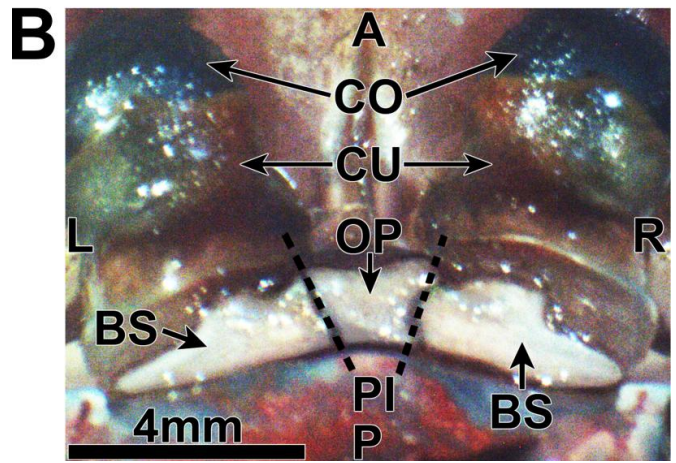
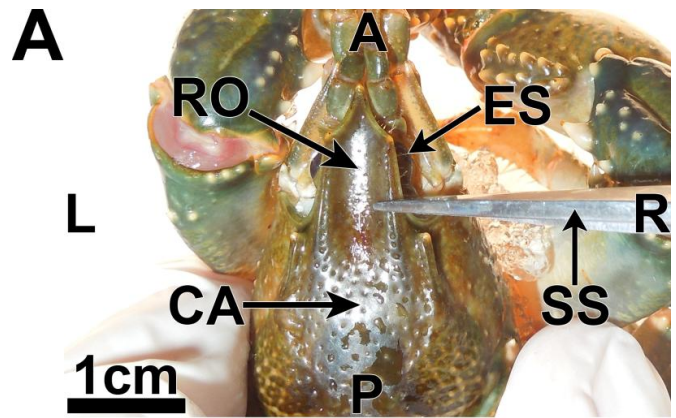


Figure 3. Rostrum removal and severing of the joint connecting the ocular plate of the protocephalon to a basal sclerite of the eyestalk. **A)** Dorsal view of the crayfish showing the location of the cut for removal of the rostrum to expose the eyestalks. **B)** Dorsal view of the exposed eyestalk. Images shown in Figs. 3B, 5A, and 5B are from *Procambarus clarkii*. The location of the joint is more apparent than in *Orconectes immunis* (cf. Discussion). A, anterior; P, posterior; L, left; R, right; ES, eyestalk; CA, carapace; RO, rostrum; SS, small dissection scissors; CO, cornea; CU, cuticle of the eye; OP, ocular plate of the protocephalon; BS, basal sclerite of the eyestalk; PI, potential incisions (represented as two dotted lines).

before placing the crayfish into a glass dissection dish (Fig. 5A). The crayfish was surrounded by ice leaving the dorsal surface of the eyestalk exposed for placement of the recording electrode and for stimulation by light (Video 1.6). With the aid of a Leica GZ6 boom stereoscope, a tungsten microelectrode was inserted through the incision that was made separating the ocular plate of the protocephalon and basal sclerite of the eyestalk. The electrode was carefully advanced using a micromanipulator into the dorsal anterior portion of the optic nerve (Fig. 5B; Video 1.7).

Proper positioning of the electrode was confirmed after noticeable responses to light. Once responses were stable and robust, the preparation was allowed to dark adapt for 20 min. Activities were then recorded in response to repeated presentations of the LED bulb (Video 1.8). The light was shuttered on for several seconds at a time separated by dark conditions of equal or greater extent.

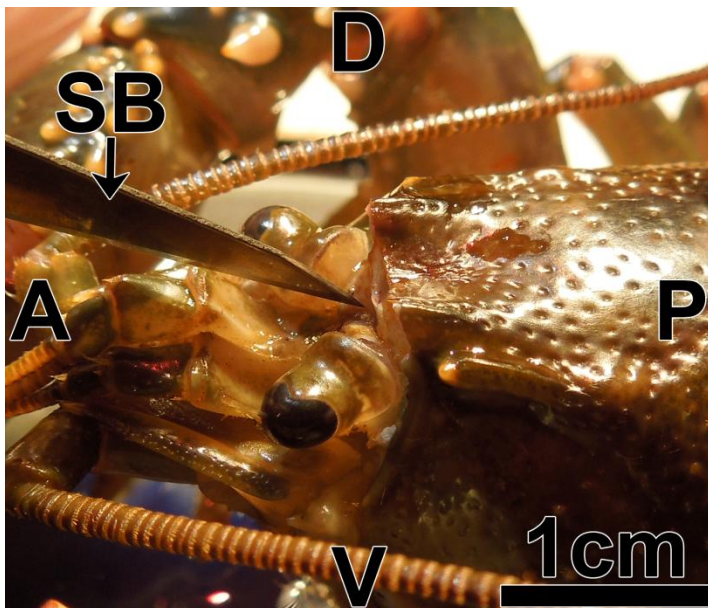


Figure 4. Left side view showing the position of the scalpel for cutting the joint of the ocular plate of the protocephalon and a basal sclerite of the eyestalk. A, anterior; P, posterior; D, dorsal; V, ventral; SB, surgical blade.

Caudal Photoreceptor

The abdomen was taken next for dissection of the caudal photoreceptor (cf. Wyttanbach et al., 2014). The abdomen with the ventral surface facing upward was pinned to Sylgard[®] mounting material (Dow Corning, Midland, MI) in the bottom of a dissection dish (Video 2.1). Four pins were used to secure the tail to the dish. Two dissection pins were used to puncture the anterior end of the tergum, one at each lateral edge. The other two pins were punctured through each of the exopodites. The dissection dish was filled with crayfish saline until the abdomen, excluding the swimmerets, was fully submerged. The mixture of 95% O₂ and 5% CO₂ was bubbled directly into the dish throughout the dissection to help preserve the preparation. Each swimmeret was then removed by holding the distal end with forceps and cutting the proximal end with microscissors (Fig. 6; Video 2.2).

After all of the swimmerets were removed, a sternite was dissected to expose part of the ventral nerve cord. A surgical blade was used to make a superficial transverse incision in the integument at either the anterior or the posterior edge of a sternite anterior to the fifth abdominal sternite (cf. Video 2.3 to Fig. 7). The incision was made at a shallow angle to avoid damaging the ventral nerve cord. Microscissors were then used to cut the sternite at the lateral edges of the incision (Fig. 8; Video 2.4). The microscissors were held at shallow angles and kept parallel to the median sagittal plane so that the lower blade stayed superficial and away from the ventral nerve cord during cutting.

The medial section of the sternite was pulled away with Dumont forceps (Fig. 9, Video 2.5). A surgical blade was used to carefully cut any connective tissue still anchoring the integument to the ventral nerve cord. Superficial coronal cuts were made with the surgical blade to help fold

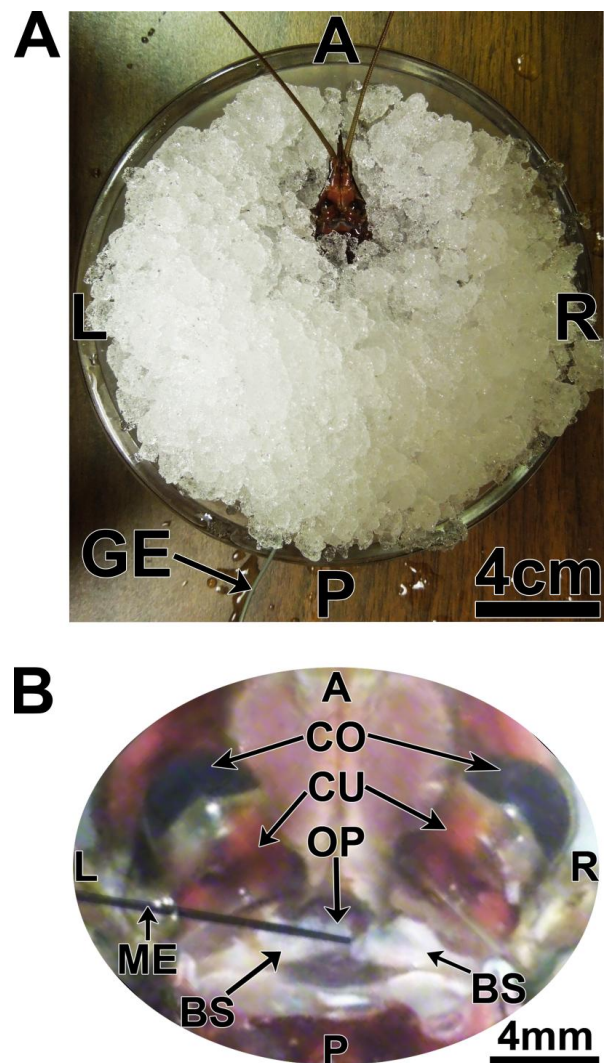


Figure 5. Anesthetizing the crayfish and recording from its optic nerve. A) Dorsal view showing the position of crayfish in ice during recording. B) Dorsal view of the eyestalk with a tungsten microelectrode inserted through the incision to record from the optic nerve fibers. A, anterior; P, posterior; L, left; R, right; GE, ground electrode; CO, cornea; CU, cuticle of the eye; OP, ocular plate of the protocephalon; BS, basal sclerite of the eyestalk; ME, tungsten microelectrode.

back the integument. If the integument did not stay folded back, then it was carefully removed by making a transverse cut with microscissors. A reference electrode was pinned in the Sylgard[®] mounting material at the bottom of the dissection dish (Video 2.6). A tungsten microelectrode tip was then inserted onto the ventral nerve cord anterior to the sixth abdominal ganglion (Kondah and Hisada, 1986) to record from the axon of the caudal photoreceptor (Video 2.7, cf. to Fig. 10, which shows the electrode inserted instead at the location of the caudal photoreceptor cell body ipsilateral to the axon; Sullivan and Herberholz, 2013). Recording from the axon or cell body of the caudal photoreceptor was confirmed after observing noticeable responses to light. As was done with optic nerve fibers, once responses were stable and robust, the preparation was allowed to dark adapt for 20 min. Activity was recorded in response to the LED bulb for several seconds

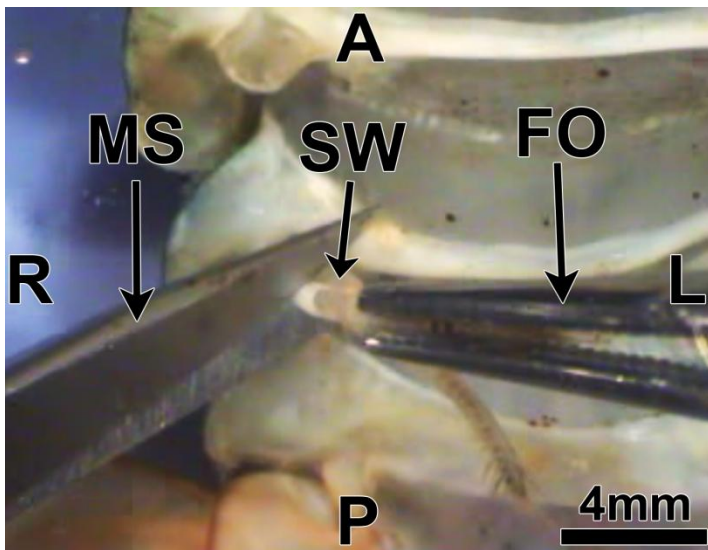


Figure 6. Ventral view of the crayfish abdomen showing the technique for swimmeret removal. A, anterior; P, posterior; L, left; R, right; SW, swimmeret; FO, forceps; MS, microscissors.

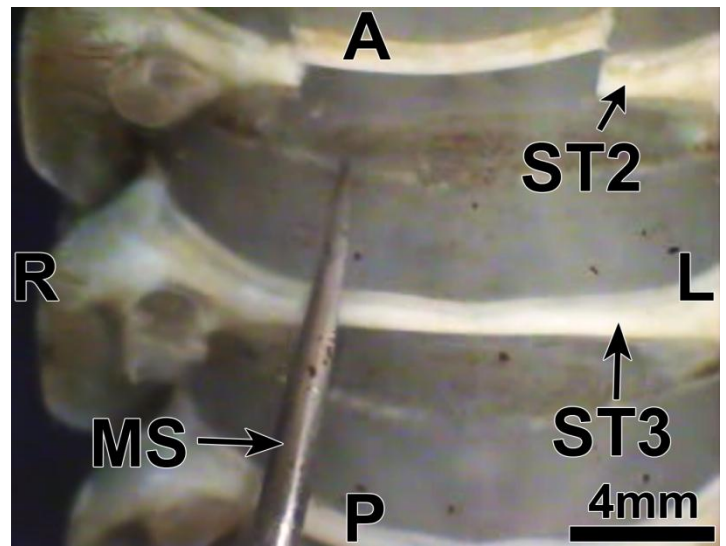


Figure 8. Ventral view showing the sternites being cut with microscissors. A, anterior; P, posterior; L, left; R, right; ST2, second abdominal sternite; ST3, third abdominal sternite; MS, microscissors.

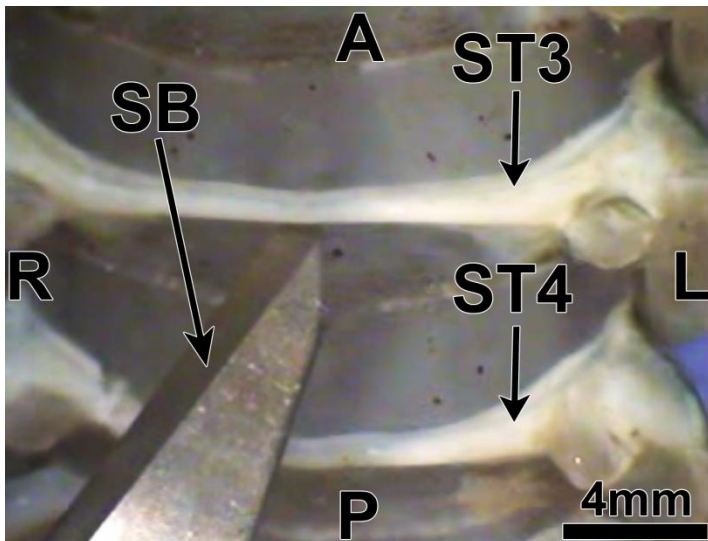


Figure 7. Ventral view showing the technique for cutting the integument at the posterior edge of the third abdominal sternite (ST3). A, anterior; P, posterior; L, left; R, right; ST4, fourth abdominal sternite; SB, surgical blade.

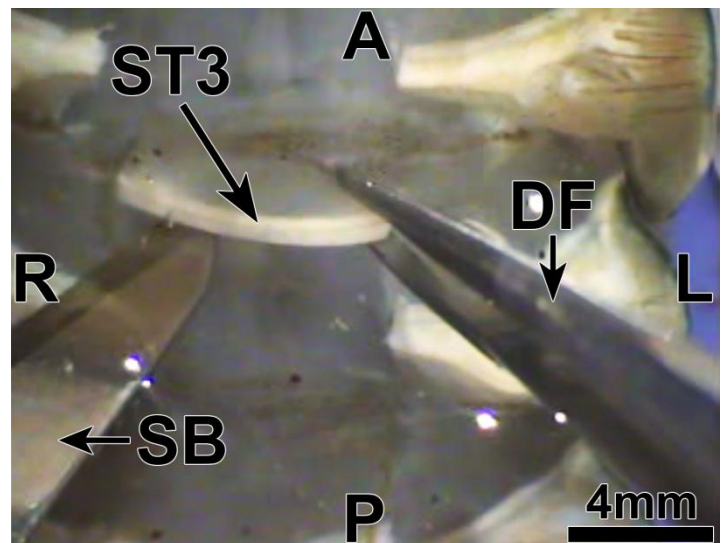


Figure 9. Ventral view showing the integument being pulled away using Dumont forceps while carefully cutting with a surgical blade. A, anterior; P, posterior; L, left; R, right; ST3, third abdominal sternite; DF, Dumont forceps; SB, surgical blade.

at a time separated by dark conditions of equal or greater extent (Video 2.8).

Analysis by LabChart®

Raw data were exported from LabChart® to MATLAB® (The MathWorks, Inc., Natick, MA) to make traces of spike activities. For a detailed description of the procedure used to measure neural firing rates in LabChart®, see [Supplementary Material](#). The frequency measurements obtained before the shutter switch was opened were referred to as dark condition firing rates. The frequency measurements obtained after the shutter was opened were the firing rates during the light condition. Firing rates were then analyzed in SPSS (IBM Corporation, Armonk, NY) to compute means and perform statistical analysis. Paired-

samples t-tests were used to compare means between firing rates. P values less than 0.05 were used to determine significant differences. Bar plots were generated using Excel (Microsoft Corporation, Redmond, WA).

RESULTS

Examples of traces of spike activities are shown for optic nerve fibers in Figure 11A and for the caudal photoreceptor in Figure 11B. Latencies of responses from optic nerve fibers were about 75 msec; latency for the caudal photoreceptor was much longer, between 2 and 3 sec.

Mean firing rates during 5 sec of dark and then 5 sec of light were determined from five repeated presentations.

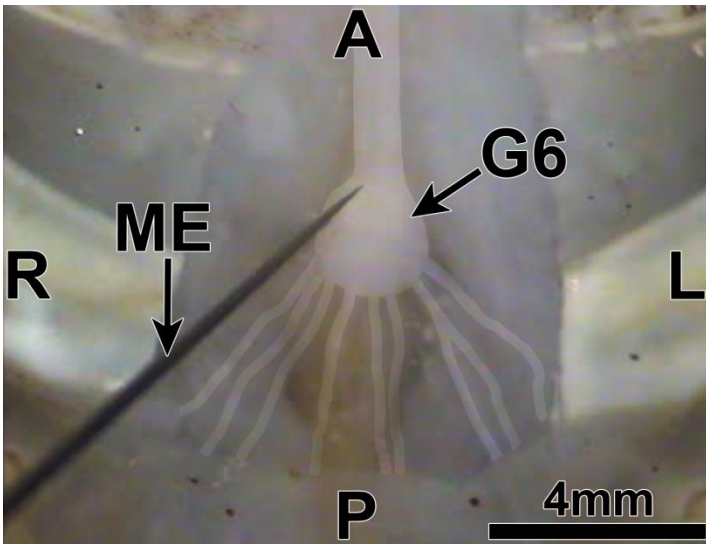


Figure 10. Ventral view of the sixth abdominal ganglion (G6) of the ventral nerve cord. The tip of the tungsten microelectrode (ME) is inserted at the location of the cell body of a caudal photoreceptor. A, anterior; P, posterior; L, left; R, right. Images here and those shown in Figures 6 through 9 are from *Orconectes immunis*, which have integument and connective tissue on the ventral side in the tail that is lighter and somewhat transparent in comparison to *Procambarus clarkii*, making the ventral nerve cord easier to see during dissection (cf. Discussion).

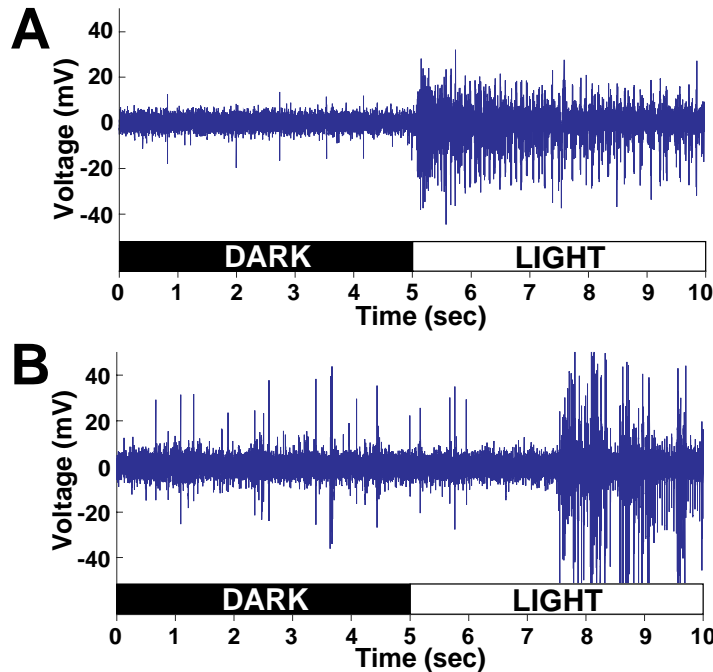


Figure 11. Spike activities during conditions of dark followed by light. A) For optic nerve fibers. B) For caudal photoreceptor.

This was done from one preparation each of the optic nerve fibers and the caudal photoreceptor. Mean firing rate calculated for optic nerve fibers (Fig. 12A) is shown compared to caudal photoreceptor (Fig. 12B). Firing rate by optic nerve fibers was greater than caudal photoreceptor as indicated by different Y-axis scales. The

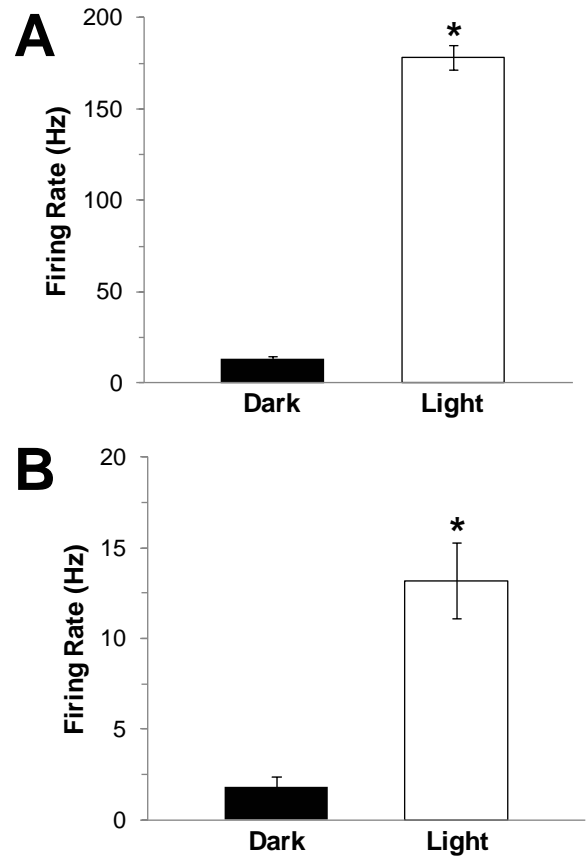


Figure 12. Mean firing rates during the dark (black) and light (white) conditions from five light presentations. A) For optic nerve fibers. B) For caudal photoreceptor. Vertical bars are standard error. Asterisk denotes statistical significance at $p < 0.05$.

mean firing rate of the optic nerve fibers during the dark condition was 13 ± 1.3 Hz and was much lower than the rate during the light condition; 178 ± 6.7 Hz. For the caudal photoreceptor, the mean firing rate during the dark condition was 2 ± 0.6 Hz. The rate also was lower than during the light condition at 13 ± 2.1 Hz. As expected, a significant difference in the firing rates was observed during the dark versus light conditions for both optic nerve fibers ($t = 22, p < 0.01$) and the caudal photoreceptor ($t = 6.7, p < 0.01$).

DISCUSSION

Different Light Responses

Students will see very different light responses from optic nerve fibers compared to the caudal photoreceptor. Image-forming functions processed by optic nerve fibers, such as identifying the location of predators or prey, need to be conveyed rapidly to the brain. In contrast, those involved in non-image-forming functions done by the caudal photoreceptor, such as detecting light cues signaling the time of the day, can be carried out more slowly. Figure 11 supports this, showing that the caudal photoreceptor has a latency of response that is more than ten times longer than that of the optic nerve fibers. The point to make to students is that this occurs when the same

light intensity is used so the difference must be due to different physiologies.

Once students understand the neural circuitries that converge on these interneurons and what is known of the physiology underlying the responses, the difference in the latencies becomes even more dramatic. Optic nerve fibers are excited by phototransduction that originates in the retinal photoreceptors of the ommatidia. Light information must be conveyed via a series of synapses beginning at the photoreceptor terminals of the compound eye then through the neuropils (lamina, medulla externa, medulla interna, and medulla terminalis) of the optic lobes, ultimately projecting via the optic nerve fibers to the lateral protocerebrum of the brain (Wang-Bennett et al., 1989; Yagodin et al., 1999; Glantz and Miller, 2002; Sullivan and Herberholz, 2013; Glantz, 2014). Caudal photoreceptors, on the other hand, directly respond to light via their dendrites; thus, there is no prior synapse relaying light information from the environment (Sullivan and Herberholz, 2013). Therefore, optic nerve fibers, even with the synaptic delays, are physiologically faster and better suited to handle image-forming processes. Caudal photoreceptors, on the contrary, with no synaptic delays, are much slower at transmitting their non-image-forming signals to the brain.

The reason for the longer latency by the caudal photoreceptor was proposed long ago to be due to a lower sensitivity to light with a slower photoreceptive mechanism of adaptation (Prosser, 1934; Welsh, 1934); however, the details of this are not fully understood. Unlike the retinal opsin, which has been sequenced showing 53% homology to *Drosophila* rhodopsin Rh1 (Hariyama et al., 1993; Crandall and Cronin 1997), the photopigment underlying the caudal photoreceptor responses and the identities of second messengers involved in phototransduction have yet to be determined (Kruszewska and Larimer, 1993; Hafner et al., 2003; Hardie, 2006; Gotow and Nishi, 2008; Rodríguez-Sosa et al., 2012). Although not identified, it is clear from the studies that the compound eye and caudal photoreceptor use different photopigments. The different spectral sensitivities measured for the eye and caudal photoreceptor support this (Kennedy and Bruno, 1961; Uttal and Kasprzak, 1962).

For some follow up to this, instead of using white light for stimulation, students could use a range of wavelengths to directly compare responses at different intensities to derive spectral sensitivity curves (e.g., Sipe et al., 2011, for the spectral sensitivity derivation for the photointrinsic response of the iris in the turtle). From sensitivity curves, students could then develop hypotheses for which photopigments identified, for example in the crayfish eyestalk (e.g., Zeiger and Goldsmith, 1989), have absorption spectra that best correlate with the spectral sensitivity of the optic nerve fibers. A similar approach can be used for the caudal photoreceptor.

Integration of Sensory Modalities

Both optic nerve fibers and caudal photoreceptors are also complicated by sensory integration of other modalities that are processed at locations in close proximity to where

electrodes are placed. Optic nerve fibers receive mechanoreceptive information associated with eye and head movement, somatosensory input, as well as input from a multitude of visual movement sensations (Wiersma and Yamaguchi, 1966). In addition, caudal photoreceptors are just two interneurons (one on either side of the ganglion) localized among 600 to 700 others that are processing incoming mechanoreception via the ventral nerve cord (Wiersma and Hughes, 1961; Hermann and Olsen, 1967; Wilkens and Larimer, 1976; Kondah and Hisada, 1986; Sullivan and Herberholz, 2013). A reflection of the difference in the number of cells from which activity can be recorded is shown in Figure 12 (in this case, for several visually responsive optic nerve fibers versus one caudal photoreceptor). The mean firing rate by optic nerve fibers (Fig. 12A) is more than ten times greater than that for the caudal photoreceptor (Fig. 12B). Note that this was done without any spike sorting and without attempt to identify other units that might be responsive to other modalities. For this reason too, the action potentials increasing from axons during the light are actually not known to be the same as those that were firing before spontaneously in the dark. Nonetheless, neural activities do clearly increase due to the addition of units firing that are sensitive to light (Fig. 11).

This problem opens opportunities for new investigations by students to properly address. To differentiate recorded responses that are light sensitive from those that are not, students can use spike sorting algorithms that come integrated with data acquisition systems. For example, in LabChart[®], an algorithm add-on called “Spike Histogram” is available. Using visual and tactile stimuli, which are presented together and then again separately, students can design experiments using these algorithms to separate different types of units and test hypotheses for how modalities are integrated. Students may also test the effects of various temperatures; experiments in this paper were only done at approximately 4°C. Prior studies show modulation of both interneuron types by temperature (Larimer, 1967; Glantz et al., 1995).

To aid this, fibers of similar function have been shown to cluster together in bundles, and the location of these mapped to distinct locations (Wiersma and Hughes, 1961; Wiersma and Yamaguchi, 1966). In the optic nerve, fibers responding with sustained spikes of activity to light are located in bundles superficial and dorsal in the anterior portion of the optic nerve (cf. Fig. 5B and Video 1.7). Cell bodies of caudal photoreceptors also have been mapped to the anterior ventral portion of the A6 and A7 neuromeres of the sixth ganglion (cf. Fig. 10 and Video 2.7).

Challenges of Dissections

Although dissections are straightforward, they do require students to take their time and use stereoscopes for precision. For dissection of the optic nerve fibers, this becomes important during the separation of the joint between the ocular plate of the protocephalon and a basal sclerite of the eyestalk (Fig. 3B). The same goes for the caudal photoreceptors during removal of the integument and sternites (Figs. 7, 8, and 9). Scalpel blades that cut

too deep lead to unsuccessful recordings.

Availability of different species provides a serendipitous way to deal with this. For carrying out the optic nerve fiber dissection, use of *Procambarus clarkii* is more advantageous as the joint between the ocular plate of the protocephalon and the basal sclerite of the eyestalk, where incisions must be made, is more apparent than in *Orconectes immunis* (Fig. 3B). The heavier pigmentation in the integument of *Procambarus clarkii* makes the joint easier to see. For dissection of the caudal photoreceptor, the reverse is true (Fig. 10); the dissection is easier for *Orconectes immunis*. The ventral nerve cord in *Orconectes immunis* is easier to see through the less pigmented integument of this species, thereby reducing the risk of severing it. The reason that *Orconectes immunis* has an integument with less pigment is not clear, but one possibility is that it has closer ancestry than *Procambarus clarkii* to a species that colonized caves or other dark environments (Mejía-Ortiz and Hartnoll, 2005). In any event, if students continue to have difficulty visualizing structures, contrasting agents such as methylene blue or Janus green can be added to the preparations (Wyttenbach et al., 2014).

Effectiveness of the Exercises

The methods for conducting recordings from the optic nerve fibers were developed by a freshman neuroscience major (SCN) at Lafayette College during the summer of 2014 in exchange for a paid stipend (EXCEL scholars program by the Academic Research Committee at Lafayette College). He developed a draft of the Materials and Methods section for this manuscript and presented a poster describing the technique at the 2014 Student Summer Research Poster Symposium at Lafayette College (Nesbit and Dearworth, 2014). Before this, he had learned the fundamentals for carrying out extracellular recordings while serving as a laboratory assistant for a Neurophysiology course taught during the prior spring semester. His role included helping the professor (JRDJr) set up the recording rigs for student exercises documented in *Crawdad* (Wyttenbach et al., 2014).

The methods for the caudal photoreceptor recordings were developed by a junior neuroscience major (AGV) during his taking of this same Neurophysiology course but instead for the purpose of completing a project that was required for the class. He too developed a draft of the section of the manuscript describing the methods of dissection and recording from caudal photoreceptors. During the following fall of 2014, student AGV extended his experiences from the course by taking an independent study, supervised by JRDJr, which began an investigation to look at how different types of acetylcholine receptor agonists affect activities of caudal photoreceptors (cf. Hermann and Skiles, 1969). SCN also continued to work as a paid EXCEL scholar for professor JRDJr, and during that fall collaborated with AGV. Students reviewed each other's drafts of the methods for the manuscript and then taught each other their procedures. For example, it was from these exchanges that results shown in Figures 11 and 12 were obtained. Some of the pictures were also

collected during those interactions (e.g., Fig. 10); however, most pictures and corresponding videos were captured by SCN in collaboration with visiting undergraduate student CCL from Juniata College, who is developing his expertise in digital media. Exercises also were taught to another neuroscience student, who will begin this fall (2015) to do her own independent study. She is a junior. Therefore, a total of four undergraduates were taught the exercises.

The students reported that the most difficult part was learning the dissection, i.e., the importance of taking care when making incisions and not going too deep (cf. Challenges of Dissections). Proper placement of the electrode onto units was next in rank of difficulty. Easier parts of the exercises included the use of the data acquisition system to visualize responses. Students stated that the ADInstruments' system was intuitive and user friendly.

Although there are some difficulties, it is clear that undergraduate students can carry out these exercises successfully. Evidence of the effectiveness of the exercises included the students' achievement in teaching one another the techniques and their ability to come up with new inquiries to try. Because of their success in learning, the exercises will be added into JRDJr's future course offering of Neurophysiology and a later detailed assessment of the exercises polled then.

Further Experiments

After students learn the dissection and recording procedure and then acquire an understanding of the functional topography, they can use the knowledge to develop new investigations. One such investigation may be correlating spectral sensitivities of responses to photopigment absorption spectra. Another might be to examine how other modalities in addition to light are integrated by the optic nerve fibers and the caudal photoreceptor. Or yet another might investigate how activities are affected by agonists/antagonists acting at various neurotransmitter receptors.

REFERENCES

- Aréchiga H, Rodríguez-Sosa L (1998) Circadian clock function in isolated eyestalk tissue of crayfish. *Proc R Soc Lond B Biol Sci* 265:1819-1823.
- Crandall KA, Cronin TW (1997) The molecular evolution of visual pigments of freshwater crayfishes (Decapoda: Cambaridae). *J Mol Evol* 45:524-534.
- Deyrup-Olsen I, Linder TM (1991) Use of invertebrate animals to teach physiological principles. *Adv Physiol Educ* 260:S22-S24.
- Edwards DH (1984) Crayfish extraretinal photoreception. I. behavioral and motoneuronal responses to abdominal illumination. *J Exp Biol* 109:291-306.
- Glantz RM (2008) Polarization vision in crayfish motion detectors. *J Comp Physiol [A]* 194:565-575.
- Glantz RM (2014) Visual systems of crustaceans. In: *Natural history of crustacea: nervous systems & control of behavior*, volume 3 (Derby C, Thiel M, eds) pp 535-553. New York, NY: Oxford UP.
- Glantz RM, Miller CS (2002) Signal processing in the crayfish optic lobe: contrast, motion and polarization vision. In: *The crustacean nervous system* (Wiese K, ed) pp 486-498. Berlin: Springer-Verlag.

- Glantz RM, Wyatt C, Mahncke H (1995) Directionally selective motion detection in the sustaining fibers of the crayfish optic nerve: linear and nonlinear mechanisms. *J Neurophysiol* 74:142-152.
- Gotowa T, Nishi T (2008) Simple photoreceptors in some invertebrates: physiological properties of a new photosensory modality. *Brain Res* 1225:3-16.
- Gruhn M, Rathmayer W (2002) An implantable electrode design for both chronic in vivo nerve recording and axon stimulation in freely behaving crayfish. *J Neurosci Methods* 118:33-40.
- Hafner GS, Martin RL, Tokarski TR (2003) Photopigment gene expression and rhabdom formation in the crayfish (*Procambarus clarkii*). *Cell Tissue Res* 311:99-105.
- Hardie RC (2006) Phototransduction in invertebrate photoreceptors. In: *Invertebrate vision* (Warrant E, Nilsson D, eds) pp 43-82. New York, NY: Cambridge UP.
- Hariyama T, Ozaki K, Tokunaga F, Tsukahara Y (1993) Primary structure of crayfish visual pigment deduced from cDNA. *Eur J Biochem* 315:287-292.
- Hauptman S, Curtis N (2009) Teaching laboratory neuroscience at Bowdoin: the laboratory instructor perspective. *J Undergrad Neurosci Educ* 8:A44-A49.
- Heitler WJ (2007) DataView: a tutorial tool for data analysis. Template based spike sorting and frequency analysis. *J Undergrad Neurosci Educ* 6:A1-A7.
- Hermann HT, Olsen RE (1967) Dynamic statistics of crayfish caudal photoreceptors. *Biophys J* 7:279-296.
- Hermann HT, Skiles MS (1969) Cholinergic inhibition of the crayfish caudal photoreceptor. *Comp Biochem Physiol* 31:575-588.
- Johnson BR, Wytenbach RA, Hoy RR (2014) Crustaceans as model systems for teaching neuroscience: past, present, and future. In: *Natural history of crustacea: nervous systems & control of behavior*, volume 3 (Derby C, Thiel M, eds) pp 535-553. New York, NY: Oxford UP.
- Johnson BR, Wytenbach RA, Hoy RR (2015) The crayfish caudal photoreceptor: a non-visual photoreceptor embedded in a central nervous system. *Soc Neurosci Abstr Online*. Chicago, IL.
- Kennedy D (1963) Physiology of photoreceptor neurons in the abdominal nerve cord of the crayfish. *J Gen Physiol* 46:551-572.
- Kennedy D, Bruno MS (1961) The spectral sensitivity of crayfish and lobster vision. *J Gen Physiol* 44:1089-1102.
- Kondah Y, Hisada M (1986) Neuroanatomy of the terminal (sixth abdominal) ganglion of the crayfish, *Procambarus clarkii* (Girard). *Cell Tissue Res* 243:273-288.
- Kruszewska B, Larimer JL (1993) Specific 2nd messengers activate the caudal photoreceptor of crayfish. *Brain Res* 618:32-40.
- Larimer JL (1967) The effects of temperature on the activity of the caudal photoreceptor. *Comp Biochem Physiol* 22:683-700.
- Mead K, Dearworth JR Jr, Grisham W, Herin GA, Jarrard H, Paul CA, Waldeck R, Yates J, Young J (2007) IFEL TOUR: a description of the Introduction to FUN Electrophysiology Labs Workshop at Bowdoin College, July 27-30, and the resultant faculty learning community. *J Undergrad Neurosci Educ* 5:A42-A48.
- Mejía-Ortiz LM, Hartnoll RG (2005) Modifications of eye structure and integumental pigment in two crayfish. *J Crust Biol* 25:480-487.
- Meyer-Rochow VB (2001) The crustacean eye: dark/light adaptation, polarization sensitivity, flicker fusion frequency, and photoreceptor damage. *Zool Sci* 18:1175-1197.
- Naka K, Kuwabara M (1959) Two components from the compound eye of the crayfish. *J Exp Biol* 36:51-61.
- Nesbit SC, Dearworth JR Jr (2014) Light responses from the optic nerve of *Procambarus clarkii*. 2014 Student Summer Research Poster Symposium, Lafayette College. Easton, PA.
- Olivo RF (2003) An online lab manual for neurophysiology. *J Undergrad Neurosci Educ* 2:A16-A22.
- Parfitt K (2002) Designing an effective, affordable laboratory course in neurophysiology. *Crawdad: A CD-ROM Lab Manual for Neurophysiology*. *J Undergrad Neurosci Educ* 1:R5-R6.
- Pei X, Wilkens LA, Moss F (1996) Light enhances hydrodynamic signaling in the multimodal caudal photoreceptor interneurons of the crayfish. *J Neurophysiol* 76:3002-3011.
- Prieto-Sagredo J, Fanjul-Moles ML (2001) Spontaneous and light-evoked discharge of the isolated abdominal nerve cord of crayfish *in vitro* reveals circadian oscillations. *Chronobiol Int* 18:759-765.
- Prosser CL (1934) Action potentials in the nervous system of the crayfish. II. responses to illumination of the eye and caudal ganglion. *J Cell Comp Physiol* 4:363-377.
- Rodríguez-Sosa L, Calderón-Rosete G, Anaya V, Flores G (2012) The caudal photoreceptor in the crayfish: an overview. In: *Photoreceptors: physiology, types and abnormalities* (Akutagawa E, Ozaki K, eds) pp 59-78. Hauppauge, NY: Nova Science Publishers.
- Rodríguez-Sosa L, Calderón-Rosete G, Flores G (2008) Circadian and ultradian rhythms in the crayfish caudal photoreceptor. *Synapse* 62:643-652.
- Sipe GO, Dearworth JR Jr, Selvarajah BP, Blaum JF, Littlefield TE, Fink DA, Casey CN, McDougal DH (2011) Spectral sensitivity of the photointrinsic iris in the red-eared slider turtle (*Trachemys scripta elegans*). *Vision Res* 51:120-133.
- Sullivan JM, Herberholz J (2013) Structure of the nervous system: general design and gross anatomy. In: *The natural history of the crustacean: functional morphology and diversity*, volume 1 (Watling L, Thiel M, eds) pp 451-484. New York, NY: Oxford UP.
- Uttal WR, Kasprzak H (1962) The caudal photoreceptor of the crayfish: quantitative study of responses to intensity, temporal and wavelength variables. *Proc Spring Jt Comput Conf* 21:159-169.
- Valdés-Fuentes M, Prieto-Sagredo J, Fanjul-Moles ML (2011) Crayfish brain-photocerebrum and retina show serotonergic functional relationship. *Brain Res* 1417:36-44.
- Van Harrevel A (1936) A physiological solution for fresh water crustaceans. *Proc Soc Exp Biol Med* 34:428-432.
- Wang-Bennett LT, Pfeiffer C, Arnold J, Glantz RM (1989) Acetylcholine in the crayfish optic lobe: concentration profile and cellular localization. *J Neurosci* 9:1864-1871.
- Welsh JH (1934) The caudal photoreceptor and responses of the crayfish to light. *J Cell Comp Physiol* 4:379-388.
- Welsh JH, Smith RI (1960) *Laboratory exercises in invertebrate physiology*. Minneapolis, MN: Burgess Pub Co.
- Welsh JH, Smith RI, Kammer AE (1968) *Laboratory exercises in invertebrate physiology*. Minneapolis, MN: Burgess Pub Co.
- Wiersma CAG (1958) On the functional connections of single units in the central nervous system of the crayfish, *Procambarus clarkii* Girard. *J Comp Neurol* 110:421-471.
- Wiersma CAG, Hughes GM (1961) On the functional anatomy of neuronal units in the abdominal cord of the crayfish, *Procambarus clarkii* (Girard). *J Comp Neurol* 116:209-228.
- Wiersma CAG, Yamaguchi T (1966) The neuronal components of the optic nerve of the crayfish as studied by single unit analysis. *J Comp Neurol* 128:333-358.
- Wilkens LA, Larimer JL (1972) The CNS photoreceptor of crayfish: morphology and synaptic activity. *J Comp Physiol [A]* 80:389-407.
- Wilkens LA, Larimer JL (1976) Photosensitivity in the sixth abdominal ganglion of decapod crustaceans: a comparative study. *J Comp Physiol [A]* 106:69-75.

Wytenbach RA, Johnson BR, Hoy RR (2014) *Crawdad: a CD-ROM lab manual of neurophysiology*. Sunderland, MA: Sinauer.

Yagodin S, Collin C, Alkon DL, Sheppard NF Jr, Sattelle DB (1999) Mapping membrane potential transients in crayfish (*Procambarus clarkii*) optic lobe neuropils with voltage-sensitive dyes. *J Neurophysiol* 81:334-344.

Zeiger J, Goldsmith TH (1989) Spectral properties of porphyropsin from an invertebrate. *Vision Res* 29:519-527.

Supplementary Video

A full-length video that demonstrates dissection and recording of optic nerve fibers and the caudal photoreceptor is available on YouTube and is titled "Recording from the Optic Nerve and Caudal Photoreceptor of the Crayfish." It can be found by typing the title into the search bar on YouTube or accessed directly with the following URL: https://youtu.be/X57qC6aZB_Y. Composition of the video is based on the style used in the *Crawdad* lab manual (Wytenbach et al., 2014). The video is divided into sixteen

parts, available in the description shown under the video on YouTube, which correspond to the links (Videos 1.1 through 2.8) found in the Materials and Methods section.

Received July 31, 2015; revised September 07, 2015; accepted September 18, 2015.

This work was supported by funding from the EXCEL scholars program by the Academic Research Committee at Lafayette College (SCN). A Delta Upsilon Distinguished Mentoring and Teaching Award (JRDJr) also was used to support travel and stay to attend the CrawFly workshop, which was the inspiration for this work. The authors thank Mr. L. Philip Auerbach for his assistance with the experimental setup and photography, Ms. Lisa C. Pezzino for ordering equipment, MicroProbes for their contribution to microelectrode selection, and Bruce R. Johnson (Cornell University) for his critical reading of the manuscript.

Address correspondence to: James R. Dearworth Jr., Biology Department and Neuroscience Program, 311 Kunkel Hall, Lafayette College, Easton, PA 18042 Email: dearworj@lafayette.edu

Copyright © 2015 Faculty for Undergraduate Neuroscience
www.funjournal.org